Electron-Impact Dissociation of Vibrationally-Excited Molecular Hydrogen into Neutral Fragments

Liam H. Scarlett [1],* , **Jeremy S. Savage [1]**, **Dmitry V. Fursa [1]**, **Mark C. Zammit [2]** and **Igor Bray [1]**

[1] Curtin Institute for Computation and Department of Physics and Astronomy, Curtin University, Perth, WA 6102, Australia
[2] Theoretical Division, Los Alamos National Laboratory, Los Alamos, NM 87545, USA
*   Correspondence: liam.scarlett@postgrad.curtin.edu.au

Abstract: We present convergent close-coupling (CCC) calculations of electron-impact dissociation of vibrationally-excited molecular hydrogen into neutral fragments. This work follows from our previous results for dissociation of molecular hydrogen in the ground vibrational level [Scarlett et al., Eur. Phys. J. D **72**, 34 (2018)], which were obtained from calculations performed in a spherical coordinate system. The present calculations, performed utilizing a spheroidal formulation of the molecular CCC method, reproduce the previous dissociation cross sections for the ground vibrational level, while allowing the extension to scattering on excited levels.

1. Introduction

The dissociation of molecular hydrogen by electron-impact excitation is a process of significant importance in the modeling of hydrogenic plasmas. The H_2 molecule is abundant in astrophysical gas clouds and plasmas, where molecular dissociation has implications for stellar formation and atmospheric modeling [1]. The neutral hydrogen found in the divertor region of the tokamak fusion reactors is primarily molecular. The rate at which it dissociates plays a role in determining the properties of the edge plasma, which in turn affects the performance of the core fusion plasma [2,3].

Many reaction channels lead to dissociation, which can be grouped into the following two general processes:

$$e^- + H_2 \rightarrow H_2^* + e^- \rightarrow H(n\ell) + H(n'\ell') + e^- \qquad \text{(1 - dissociation into neutral fragments)}$$
$$\rightarrow H_2^{+*} + 2e^- \rightarrow H^+ + H(n\ell) + 2e^-. \qquad \text{(2 - dissociative ionization)}$$

In this paper, we focus our attention on the first process—dissociation leading to only neutral atomic fragments. This process is challenging to study experimentally, since the detection of neutral fragments is substantially more difficult than it is for charged fragments. The only available experimental data [4] for dissociation of the ground vibrational level were obtained by subtracting the ionization cross section from Corrigan's 1965 measurements [5] of the total dissociation cross section (including Processes (1) and (2)). These measurements were performed more than 50 years ago and there have been no subsequent attempts at repeating them. For dissociation of vibrationally-excited H_2, there are no experimental data.

Theoretical estimates of dissociation cross sections are difficult due to the large number of dissociation channels which must be accounted for. In a previous paper [6], we analyzed the convergent close-coupling (CCC) results for electronic excitation of H_2 [7] to produce a cross section for

dissociation of H_2 in the ground electronic and vibrational state, finding that several hundred electronic states must be accounted for to yield a convergent dissociation cross section. Furthermore, a proper treatment of dissociation (including excitation-radiative-decay dissociation) requires collision data resolved not only in the electronic levels, but in the initial and final vibrational levels, which vastly increases the computational expense of the calculations. Prior to the CCC estimates of dissociation [6], calculations were limited to low incident energies where only a small number of reaction channels are open [8–10], or large energies where the Born approximation may be applied [11]. No attempts were made to produce a dissociation cross section including all reaction channels over a wide range of incident energies. The low-energy adiabatic-nuclei (AN) R-matrix calculations of the $X^1\Sigma_g^+ \to b^3\Sigma_u^+$ excitation by Stibbe and Tennyson [10] provide a good estimate of the dissociation cross section below approximately 12 eV (depending on the initial vibrational level), where the higher electronic states are closed. These are the only previous quantum-mechanical calculations which account for scattering on excited vibrational levels. However, due to the difficulty of performing molecular scattering calculations at large internuclear separations, the R-matrix calculations only treated scattering on the $v_i = 0–4$ vibrational levels explicitly, using an extrapolation procedure for the remaining vibrational levels [12].

Recently, the molecular CCC method has been utilized to produce cross sections for dissociative excitation [13] and excitation-radiative-decay dissociation [14], for scattering on all $v_i = 0–14$ bound vibrational levels of the ground electronic ($X^1\Sigma_g^+$) state to a number of low-lying singlet states of H_2. To allow accurate structure and scattering calculations to be performed over the range of internuclear separations spanned by the $v_i = 0–14$ vibrational levels, the CCC theory was formulated in spheroidal coordinates [15]. Here, we utilize these results, as well as calculations for excitation of vibrationally-excited H_2 into the triplet system, to produce $e^- – H_2$ dissociation cross sections for scattering on all initial vibrational levels, over the energy range from threshold to 120 eV. Atomic units are used throughout the paper unless specified otherwise.

2. Theory

Excitation-induced molecular dissociation occurs via three main mechanisms: dissociative excitation (DE), excitation-radiative-decay dissociation (ERDD), and predissociation (PD). Detailed discussions of the spheroidal molecular CCC method, and the calculations of DE and ERDD cross sections can be found in Refs. [6,13–15], thus only a brief overview is given here.

2.1. Spheroidal Molecular CCC Method

The spheroidal molecular CCC method follows the same approach as the spherical-coordinate implementation, for which a detailed discussion can be found in Ref. [16]. The principle difference is that the coordinate space of the projectile-target system is described using a system of prolate spheroidal coordinates $\boldsymbol{\rho} = (\rho, \eta, \phi)$, with

$$\rho = \frac{r_1 + r_2}{2} - \frac{R}{2} \ \text{ and } \ \eta = \frac{r_1 - r_2}{2}, \tag{1}$$

where R is the internuclear separation, and r_1 and r_2 are the distances from the two nuclei. The z-axis is aligned with the internuclear axis, and the azimuthal angle ϕ retains its definition from the spherical coordinate system. The use of spheroidal coordinates provides a significant improvement in both accuracy and efficiency when calculating the target wave functions, which are inherently non-spherical, particularly at larger values of R.

The Born–Oppenheimer approximation is utilized, allowing the electronic structure calculation to be performed independent of the nuclear motion, at fixed values of R. The target wave functions and energies are obtained by diagonalizing the fixed-nuclei electronic molecular Hamiltonian in a basis of Sturmian (Laguerre) functions, which is optimized to yield an accurate description of the low-lying

states, and an adequate pseudo-state discretization of the continuum. Specific details of the structure calculation used in the present work can be found in Ref. [15].

The projectile wave functions are expanded in partial waves of spheroidal pseudo-angular-momentum λ and angular-momentum projection m, and the total scattering wave function is expanded in terms of the asymptotic channels of the scattering system Hamiltonian. The partial-wave fixed-nuclei scattering amplitudes $F_{f\lambda_f m_f, i\lambda_i m_i}(R; E_{\text{in}})$ are obtained by solving the resulting set of coupled Lippmann–Schwinger equations at a given incident electron energy E_{in} and internuclear separation R. The number of target states and projectile partial waves included in the calculations determines the accuracy of the scattering cross sections. The present calculations utilize a scattering model consisting of 210 bound and continuum electronic (pseudo)states, which we have found to yield a sufficient level of convergence for a number of low-lying excitations. A full discussion of the scattering models we have used and the methods for obtaining the scattering amplitudes can be found in Refs. [13,15].

The adiabatic-nuclei approximation is invoked to restore the dependence on the nuclear motion, yielding cross sections for vibrationally-resolved electronic transitions $iv_i \rightarrow fv_f$:

$$\sigma_{fv_f, iv_i}(E_{\text{in}}) = \frac{q_{fv_f}}{4\pi q_i} \sum_{\substack{\lambda_f, \lambda_i \\ m_f, m_i}} \left| \langle v_{fv_f} | F_{f\lambda_f m_f, i\lambda_i m_i}(R; E_{\text{in}}) | v_{iv_i} \rangle \right|^2, \tag{2}$$

where q_{fv_f} and q_i are the outgoing and incident projectile linear momenta, and v_{nv_n} are the vibrational wave functions, which are obtained by diagonalizing the Born–Oppenheimer nuclear Hamiltonian

$$H_n^{\text{BO}} = -\frac{1}{2\mu} \frac{\mathrm{d}^2}{\mathrm{d}R^2} + \frac{J(J+1) - \Lambda_n^2}{2\mu R^2} + \epsilon_n(R), \tag{3}$$

where μ is the nuclear reduced mass, ϵ_n is the potential-energy curve of the electronic state n, J is the total molecular angular momentum, and Λ_n is the electronic-state angular momentum projection onto the internuclear axis. For the purposes of obtaining cross sections resolved in the target electronic and vibrational levels only, we may neglect the centrifugal term in Equation (3), as for small J it is negligible compared to ϵ_n.

It is worth noting that the AN cross section we define in Equation (2) includes the correct outgoing projectile momentum

$$q_{fv_f} = \sqrt{2 \left[E_{\text{in}} - \varepsilon_{fv_f, iv_i} \right]}, \tag{4}$$

where ε_{fv_f, iv_i} is the vibrationally-resolved excitation energy. The more common AN formulation (as given by Lane [17], for example) absorbs the outgoing momentum into the integral over R, in doing so replacing it with the R-dependent fixed-nuclei momentum

$$q_f(R) = \sqrt{2 \left[E_{\text{in}} - \epsilon_{f,i}(R) \right]}, \tag{5}$$

where $\epsilon_{f,i}$ is the fixed-nuclei (vertical) excitation energy. In the present notation, the resulting AN cross section is

$$\sigma_{fv_f, iv_i}(E_{\text{in}}) = \frac{1}{4\pi q_i} \sum_{\substack{\lambda_f, \lambda_i \\ m_f, m_i}} \left| \langle v_{fv_f} | \sqrt{q_f(R)} F_{f\lambda_f m_f, i\lambda_i m_i}(R; E_{\text{in}}) | v_{iv_i} \rangle \right|^2. \tag{6}$$

The latter method allows for the electronic excitation cross section (summed over final vibrational levels) to be evaluated using

$$\sigma_{f, iv_i} = \langle v_{iv_i} | \sigma_{f,i} | v_{iv_i} \rangle, \tag{7}$$

where $\sigma_{f,i}$ is the (R-dependent) FN electronic excitation cross section. In the present formulation, Equation (2) must be summed over final levels numerically, however at larger incident energies ($\approx$10 eV above the electronic excitation threshold), Equation (7) returns the same result. The present formulation in Equation (2) is convenient when partitioning excitation cross sections into the various dissociative pathways as it retains the correct vibrationally-resolved excitation thresholds, which are lost in the standard AN formulation.

2.2. Dissociative Excitation

DE is the direct impact-induced transition from the initial state iv_i to a dissociative level in the vibrational continuum of some electronic state f. Evaluation of the DE cross section formally requires integration of the kinetic-energy-release cross section $d\sigma_{f,iv_i} / dE_k$ over the kinetic energy E_k of the dissociation fragments. However, the dissociative pseudostates resulting from diagonalizing Equation (3) form a quadrature rule for integrating over the vibrational continuum, so we can equivalently sum Equation (2) over these states in the same way that ionization is typically treated in the CCC method. We have previously performed calculations for dissociative excitation of the $B^1\Sigma_u^+$, $C^1\Pi_u$, $B'^1\Sigma_u^+$, $D^1\Pi_u$, and $E,F^1\Sigma_g^+$ electronic singlet states for electrons scattering on all $v_i = 0$–14 bound vibrational levels of the H_2 ground electronic state ($X^1\Sigma_g^+$) [13].

2.3. Excitation-Radiative-Decay Dissociation

ERDD proceeds via excitation of the bound vibrational spectrum of an excited electronic state, followed by radiative decay to the dissociative vibrational continuum of a lower electronic state. The decay sequences can include multiple electronic states, and terminate in the bound spectrum of the $X^1\Sigma_g^+$ state or the vibrational continuum of either the ground or an excited electronic state. We have adopted the following approach [14] for obtaining the ERDD cross section for an electronic state f: we calculate the excitation-radiative-decay cross section for decays back to the bound vibrational levels of the ground electronic state

$$\sigma_{iv_i',f,iv_i}^{\text{ERD}} = (1 - F_{f,iv_i}^{\text{PD}}) \sum_{v_f} \frac{A_{i,f}(v_i', v_f)}{A_f(v_f)} \sigma_{fv_f,iv_i} \tag{8}$$

and subtract it from the cross section for excitation of the bound levels of state f, giving

$$\sigma_{i,f,iv_i}^{\text{ERDD}} = (1 - F_{f,iv_i}^{\text{PD}}) \sum_{v_f} \left(1 - \sum_{v_i'} \frac{A_{i,f}(v_i', v_f)}{A_f(v_f)} \right) \sigma_{fv_f,iv_i}. \tag{9}$$

In Equations (8) and (9), $A_{i,f}(v_i', v_f)$ is the $fv_f \rightarrow iv_i'$ radiative transition probability, $A_f(v_f)$ is the total transition probability for the state fv_f, and F_{f,iv_i}^{PD} is the fraction of the excitation cross section σ_{f,iv_i} which leads to PD. We have previously performed calculations of excitation-radiative-decay dissociation for the $B^1\Sigma_u^+$, $C^1\Pi_u$, $B'^1\Sigma_u^+$, $D^1\Pi_u$, and $E,F^1\Sigma_g^+$ electronic singlet states, for electrons scattering on all $v_i = 0$–14 bound vibrational levels of the $X^1\Sigma_g^+$ state [14].

2.4. Constructing the Dissociation Cross Section

The contribution from the electronic singlet spectrum to the total neutral-fragment dissociation cross section is the sum of the DE, ERDD, and PD processes for all electronically bound (i.e., non-ionizing) singlet states. For the $B^1\Sigma_u^+$, $C^1\Pi_u$, $B'^1\Sigma_u^+$, $D^1\Pi_u$, and $E,F^1\Sigma_g^+$ states we use the CCC DE and ERDD cross sections which have been previously calculated [13,14]. PD does not occur or is negligible for these states, except for the $D^1\Pi_u$ state. We take the PD fraction of 0.2564 for the $D^1\Pi_u$ state from Glass-Maujean et al. [18]. To approximately account for dissociation through the remaining singlet states, we obtain an effective dissociation fraction for the states we have considered explicitly

by summing their respective dissociation cross sections and dividing by their summed excitation cross section. We then apply this dissociation fraction to each of the remaining excited bound electronic states. The same approach to approximately accounting for higher excited singlet states was used in our previous calculations of dissociation from the ground vibrational level [6]. Although dissociation may also proceed through direct excitation of the $X^1\Sigma_g^+$ vibrational continuum, we have found that the cross sections for this process are two orders of magnitude smaller than the $b^3\Sigma_u^+$ DE cross section for scattering on the same initial vibrational level, and are therefore neglected.

Dissociation through the triplet spectrum is simpler to analyse. Assuming an *L-S* coupling scheme, radiative transitions between the triplet spectrum and the singlet ground state are spin forbidden. Since the lowest triplet state of H_2 ($b^3\Sigma_u^+$) is purely repulsive, excitation of any triplet state must eventually result in dissociation. The cross section for dissociation through the triplet spectrum is then simply the sum of all electronically bound triplet-state excitations.

Stibbe and Tennyson [10] proposed an *energy-balancing* modification to the AN method, which more accurately treats the partitioning of energies between the outgoing electron and dissociation fragments. The technique requires evaluating the fixed-nuclei scattering amplitudes at a modified *R*-dependent incident energy

$$E(R) = E_{\text{in}} - \varepsilon_{fv_f,iv_i} + \epsilon_{f,i}(R). \tag{10}$$

This definition ensures that at every value of R the fixed-nuclei outgoing momentum $q_f(R)$ is equal to the physical outgoing momentum q_{fv_f} (Equations (4) and (5) are equivalent when E_{in} is replaced by $E(R)$ in Equation (5)). In the present notation, the energy-balanced cross section is

$$\sigma_{fv_f,iv_i}^{\text{e bal}}(E_{\text{in}}) = \frac{q_{fv_f}}{4\pi q_i} \sum_{\substack{\lambda_f,\lambda_i \\ m_f,m_i}} \left| \langle v_{fv_f} | F_{f\lambda_f m_f, i\lambda_i m_i}(R; E(R)) | v_{iv_i} \rangle \right|^2. \tag{11}$$

Stibbe and Tennyson [10] applied this technique to the dissociative $b^3\Sigma_u^+$ excitation using true continuum nuclear functions for the final vibrational levels, and integrating over the fragments kinetic energy to obtain integral DE cross sections. As the $b^3\Sigma_u^+$ excitation is the primary dissociation channel at low energies we utilize the energy-balancing technique for this transition, but rather than integrating the kinetic-energy-release cross section we equivalently sum Equation (11) over final vibrational pseudostates until convergence is reached. For the remaining triplet states, a less accurate approach is sufficient, and we utilize the analytical sum over final vibrational levels in Equation (7) to give

$$\sigma_{iv_i}^{\text{rem. trip.}} = \langle v_{iv_i} | \sum_f \sigma_{f,i} | v_{iv_i} \rangle, \tag{12}$$

where the sum is over all bound electronic triplet states above the $b^3\Sigma_u^+$ state.

3. Results

In Figure 1, we present the cross sections for excitation of the $b^3\Sigma_u^+$ state from all bound vibrational levels in the $X^1\Sigma_g^+$ state. This transition is the dominant dissociative process within the triplet system, and the dominant overall dissociative process at low energies. The cross section is substantially enhanced at low energies when scattering on excited vibrational levels. This enhancement is due to the degeneracy of the $X^1\Sigma_g^+$ and $b^3\Sigma_u^+$ states at larger internuclear separations, which results in small excitation energies for transitions from the high-lying vibrational levels of the ground state to the dissociative levels of the $b^3\Sigma_u^+$ state. As shown by Trevisan and Tennyson [19,20], a significant portion of the energy required to excite this transition is carried away by the dissociation fragments. The large cross section for this process (particularly for low-energy electrons scattering on excited

vibrational levels) then corresponds to the release of significant quantities of hot H atoms into the plasma or other medium.
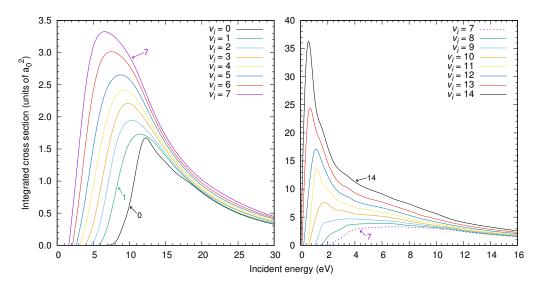

Figure 1. Electron-impact cross sections for excitation from the $v_i = 0$–14 vibrational levels of the $X^1\Sigma_g^+$ state to the dissociative $b^3\Sigma_u^+$ state of H_2. The cross sections increase monotonically with increasing v_i.

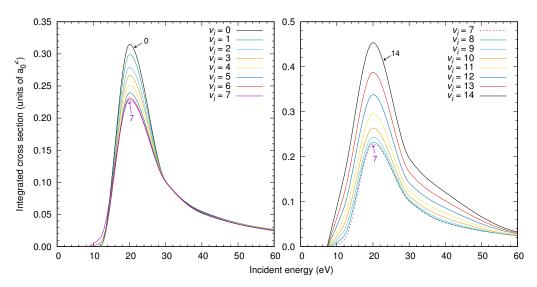The summed cross section for excitation of the remaining triplet states is presented in Figure 2.

Figure 2. Electron-impact cross sections for excitation from the $v_i = 0$–14 vibrational levels of the $X^1\Sigma_g^+$ state to the bound electronic triplet spectrum of H_2 (minus the $b^3\Sigma_u^+$ state). The cross sections decrease with increasing v_i up to $v_i = 7$ (**left**), and rise with increasing v_i for $v_i > 7$ (**right**).

The remaining-triplet cross section is qualitatively similar to the $b^3\Sigma_u^+$ cross section for scattering on the ground vibrational level, but does not exhibit the low-energy spike for scattering on high vibrational levels, due to the electronic separation of the $X^1\Sigma_g^+$ state from the triplet spectrum above the $b^3\Sigma_u^+$ state. For the same reason, the cross sections for excitation of the remaining triplet states show a much smaller dependence on the initial vibrational level than the $b^3\Sigma_u^+$ excitation.

The contribution to the dissociation cross section from the singlet spectrum is presented in Figure 3. These results are the sum of the DE and ERDD cross sections published previously [13,14] for the $B^1\Sigma_u^+$, $C^1\Pi_u$, $B'^1\Sigma_u^+$, $D^1\Pi_u$, and $E, F^1\Sigma_g^+$ states, plus the estimate of PD through the $D^1\Pi_u$ state, and the estimate of dissociation through the remaining singlet states (as discussed in Section 2.4).
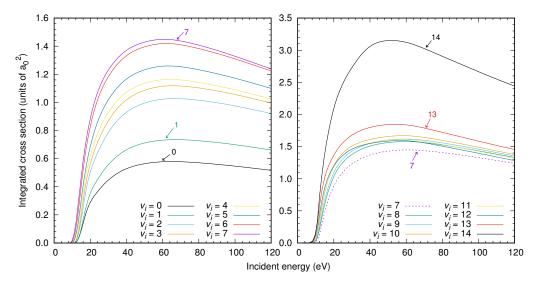
Figure 3. Electron-impact cross sections for dissociation of the $v_i = 0$–14 vibrational levels of the $X^1\Sigma_g^+$ state through the singlet spectrum of H_2.

The total neutral-fragment dissociation cross section is obtained by summing the above results for dissociation through the triplet and singlet spectra. For scattering on the ground vibrational level, we find agreement between the present results and our previous calculations [6] which were performed using converged (491-state) spherical-coordinate fixed-nuclei cross sections weighted with dissociation fractions obtained from a smaller (27-state) spheroidal adiabatic-nuclei model. In Figure 4, we compare the present (210-state) and previous (410-state) calculations with the recommended cross section of Yoon et al. [4]. The agreement between the two CCC results demonstrates that the present model yields sufficient convergence in the dissociation cross section. As we noted in our previous work [6], the substantial (up to a factor of 2) disagreement between the recommended data and the CCC results between 15 and 60 eV highlights the need for new measurements to be taken to clarify the situation.
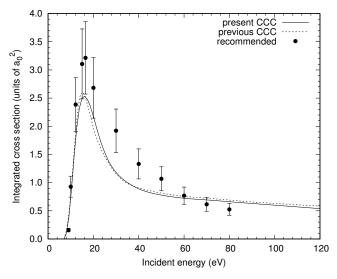

Figure 4. Electron-impact dissociation cross section for scattering on the ground (electronic and vibrational) level of H_2, comparing the present results with our previous calculations [6] and the recommended cross sections of Yoon et al. [4].

In Figure 5, we present the CCC results for dissociation of all $v_i = 0$–14 vibrational levels of the $X^1\Sigma_g^+$ state into neutral fragments. At low energies, the dissociation cross section is entirely comprised of the $b^3\Sigma_u^+$ excitation. The unusual shapes present in some curves are the result of higher

electronic-state excitations becoming open as the incident energy increases. Over the entire energy range, the dissociation cross sections are significantly enhanced for scattering on excited vibrational levels, illustrating the importance of vibrationally-resolved collision data for modeling environments where molecules are present in vibrationally-excited states, such as fusion plasmas.
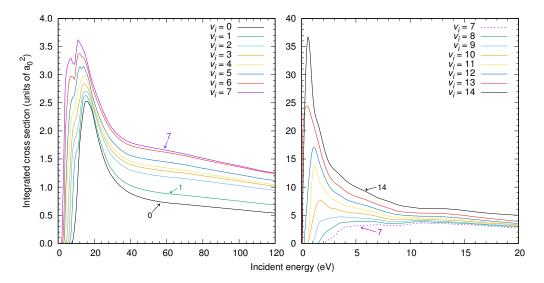

Figure 5. Electron-impact dissociation cross section for scattering on all bound vibrational levels of the H_2 ground electronic state. The cross sections rise monotonically with increasing vibrational level v_i.

The approximate way in which we have treated dissociation through the higher excited singlet states introduces an uncertainty in the dissociation results we have presented here. To provide the most liberal estimate, we allow for a 100% uncertainty in the contribution from the these singlets. We also estimate an overall uncertainty u_{CCC} of approximately 10% in the underlying CCC excitation cross sections, due to convergence and target structure accuracy. The combined uncertainty $u = \sqrt{u_{singlets}^2 + u_{CCC}^2}$ is presented in Figure 6 as a function of incident energy and initial vibrational level. For scattering on the $v_i = 0$–7 vibrational levels, the present results have an uncertainty no greater than 15%, and up to $v_i = 12$ the uncertainty is less than 20%.
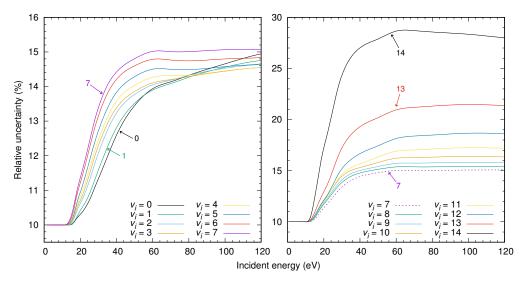

Figure 6. Relative uncertainty in the CCC dissociation cross section for each initial vibrational level.

4. Conclusions

We have presented a set of cross sections for electron-impact dissociation of vibrationally-excited H_2 into neutral fragments. An accurate treatment of the major dissociative mechanisms requires a fully vibrationally-resolved description of the e^-–H_2 scattering problem, which is made possible with the formulation of the molecular CCC method in spheroidal coordinates. For scattering on the ground vibrational level, the CCC results predict a substantially lower dissociation cross section than the only available experimental data in the 15–60 eV energy range [4,5], while for scattering on excited levels there are no available experimental data. We hope the present calculations, which represent the only available dissociation estimates for all initial vibrational levels over a wide range of incident energies, will be of interest for modeling fusion and astrophysical plasmas where molecular hydrogen is found in a range of vibrationally excited states.

Author Contributions: Methodology, L.H.S., J.S.S., M.C.Z., D.V.F. and I.B; writing–original draft preparation, L.H.S; writing–review and editing, L.H.S., J.S.S., M.C.Z., D.V.F. and I.B.

Conflicts of Interest: The authors declare no conflict of interest.

References

1. Liu, X.; Ahmed, S.M.; Multari, R.A.; James, G.K.; Ajello, J.M. High-resolution electron-impact study of the far-ultraviolet emission spectrum of molecular hydrogen. *Astrophys. J. Suppl. Ser.* **1995**, *101*, 375–399. [CrossRef]
2. Sawada, K.; Fujimoto, T. Effective ionization and dissociation hydrogen in plasma. *J. Appl. Phys.* **1995**, *78*, 2913–2924. [CrossRef]
3. Jonin, C.; Liu, X.; Ajello, J.M.; James, G.K.; Abgrall, H. High resolution electron-impact emission spectrum of H_2. I. Cross sections and emission yields 900–1200 Å. *Astrophys. J. Suppl. Ser.* **2000**, *129*, 247–266. [CrossRef]
4. Yoon, J.S.; Song, M.Y.; Han, J.M.; Hwang, S.H.; Chang, W.S.; Lee, B.; Itikawa, Y. Cross Sections for Electron Collisions with Hydrogen Molecules. *J. Phys. Chem. Ref. Data* **2008**, *37*, 913–931. [CrossRef]
5. Corrigan, S.J.B. Dissociation of Molecular Hydrogen by Electron Impact. *J. Chem. Phys.* **1965**, *43*, 4381. [CrossRef]
6. Scarlett, L.H.; Tapley, J.K.; Fursa, D.V.; Zammit, M.C.; Savage, J.S.; Bray, I. Electron-impact dissociation of molecular hydrogen into neutral fragments. *Eur. Phys. J. D* **2018**, *72*, 34. [CrossRef]
7. Zammit, M.C.; Savage, J.S.; Fursa, D.V.; Bray, I. Electron-impact excitation of molecular hydrogen. *Phys. Rev. A* **2017**, *95*, 022708. [CrossRef]
8. Chung, S.; Lin, C.C. Application of the close-coupling method to excitation of electronic states and dissociation of H_2 by electron impact. *Phys. Rev. A* **1978**, *17*, 1874–1891. [CrossRef]
9. Borges, I.; Jalbert, G.; Bielschowsky, C.E. Non-Franck-Condon electron-imact dissociative-excitation cross sections of molecular hydrogen producing $H(1s) + H(2l)$ through $X^1\Sigma_g^+ (v = 0) \rightarrow \{B^1\Sigma_u^+, B'^1\Sigma_u^+, C^1\Pi_u\}$. *Phys. Rev. A* **1998**, *57*, 1025–1032. [CrossRef]
10. Stibbe, D.T.; Tennyson, J. Near-threshold electron impact dissociation of H_2 within the adiabatic nuclei approximation. *New J. Phys.* **1998**, *1*, 2. [CrossRef]
11. Liu, X.; Shemansky, D.E.; Johnson, P.V.; Malone, C.P.; Khakoo, M.A.; Kanik, I. Electron and photon dissociation cross sections of the H_2 singlet ungerade continua. *J. Phys. B At. Mol. Opt. Phys.* **2012**, *45*, 105203. [CrossRef]
12. Stibbe, D.T.; Tennyson, J. Rates for the electron impact dissociation of molecular hydrogen. *Astrophys. J.* **1999**, *513*, 147–150. [CrossRef]
13. Tapley, J.K.; Scarlett, L.H.; Savage, J.S.; Fursa, D.V.; Zammit, M.C.; Bray, I. Electron-impact dissociative excitation of singlet states of molecular hydrogen. *Phys. Rev. A* **2018**, *98*, 032701. [CrossRef]

14. Scarlett, L.H.; Tapley, J.K.; Savage, J.S.; Fursa, D.V.; Zammit, M.C.; Bray, I. Vibrational excitation of the H_2 $X^1\Sigma_g^+$ state via electron-impact excitation and radiative cascade. *Plasma Sources Sci. Technol.* **2019**, *28*, 025004. [CrossRef]

15. Tapley, J.K.; Scarlett, L.H.; Savage, J.S.; Zammit, M.C.; Fursa, D.V.; Bray, I. Vibrationally resolved electron-impact excitation cross sections for singlet states of molecular hydrogen. *J. Phys. B At. Mol. Phys.* **2018**, *51*, 144007. [CrossRef]

16. Zammit, M.C.; Fursa, D.V.; Savage, J.S.; Bray, I. Electron– and positron–molecule scattering: Development of the molecular convergent close-coupling method. *J. Phys. B At. Mol. Opt. Phys.* **2017**, *50*, 123001. [CrossRef]

17. Lane, N.F. The theory of electron-molecule collisions. *Rev. Mod. Phys.* **1980**, *52*, 29–119. [CrossRef]

18. Glass-Maujean, M.; Liu, X.; Shemansky, D.E. Analysis of Electron-Impact Excitation and Emission of the $np\sigma^1\Sigma_u^+$ and $np\pi^1\Pi_u$ Rydberg Series of H_2. *Astrophys. J. Suppl. Ser.* **2009**, *180*, 38. [CrossRef]

19. Trevisan, C.S.; Tennyson, J. Differential cross sections for near-threshold electron impact dissociation of molecular hydrogen. *J. Phys. B At. Mol. Opt. Phys.* **2001**, *34*, 2935–2949. [CrossRef]

20. Trevisan, C.; Tennyson, J. Calculated rates for the electron impact dissociation of molecular hydrogen, deuterium and tritium. *Plasma Phys. Control. Fusion* **2002**, *44*, 1263–1276. [CrossRef]